

Experimental and numerical investigation on in-plane behaviour of hollow concrete block masonry panels

A. Rama Chandra Murthy*, S. Chitra Ganapathi, Nagesh R. Iyer,
N. Lakshmanan and N.G. Bhagavan

CSIR-Structural Engineering Research Centre, CSIR Campus, Taramani, Chennai-600 113, India

(Received June 16, 2010, Revised January 13, 2011, Accepted June 22, 2011)

Abstract. This paper presents the details of studies conducted on hollow concrete block masonry (HCBM) units and wall panels. This study includes, compressive strength of unit block, ungrouted and grouted HCB prisms, flexural strength evaluation, testing of HCBM panels with and without opening. Non-linear finite element (FE) analysis of HCBM panels with and without opening has been carried out by simulating the actual test conditions. Constant vertical load is applied on the top of the wall panel and then lateral load is applied in incremental manner. The in-plane deformation is recorded under each incremental lateral load. Displacement ductility factors and response reduction factors have been evaluated based on experimental results. From the study, it is observed that fully grouted and partially reinforced HCBM panel without opening performed well compared to other types of wall panels in lateral load resistance and displacement ductility. In all the wall panels, shear cracks originated at loading point and moved towards the compression toe of the wall. The force reduction factor of a wall panel with opening is much less when compared with fully reinforced wall panel with no opening. The displacement values obtained by non-linear FE analysis are found to be in good agreement with the corresponding experimental values. The influence of mortar joint has been included in the stress-strain behaviour as a monolith with HCBM and not considered separately. The derived response reduction factors will be useful for the design of reinforced HCBM wall panels subjected to lateral forces generated due to earthquakes.

Keywords: hollow concrete block masonry; prisms; wall panels; ductility; finite element analysis; static nonlinear.

1. Introduction

In masonry buildings, structural walls are principally designed to resist gravity loads. Horizontal loads, induced by earthquakes, generate large in-plane and out-of-plane forces in the walls. The damage phenomena of masonry buildings under seismic forces is very complex due to cyclic action of inertia dependent lateral loads, distribution of forces from roof/floor (rigid or flexible diaphragm) to shear walls (direction dependent with respect to ground motion), influence of soil and foundation with respect to peak ground acceleration levels, seismic energy input into the structural system at dominant frequency of structural system, use of unconventional structural elements and geometry of building, use of locally available materials in the construction and an use of unskilled labour. The shear walls of a masonry building under lateral loading generally experience two types of failures. The first one is in-plane failure, generally characterised by a diagonal tensile crack. The second one

* Corresponding author, Scientist, E-mail: murthyarc@serc.res.in

is out-of-plane failure, where cracks appear along the horizontal mortar joints.

Seismic resistance design of masonry buildings requires reinforced masonry construction to prevent sudden collapse and minimize damage. Many dwellings can be economically safeguarded by adopting confined masonry construction. The importance of reinforcement in brick or hollow block masonry with tie columns and bands has not been much understood. The masonry wall with fewer joints is also superior compared with a wall with more joints because the strength of the wall is often governed by the mortar strength. The low tensile strength characteristics and brittle failure modes of masonry panels under shear are still the basic uncertain parameters to effectively use the unreinforced masonry panels as shear panels for the seismic-resistant design of low-rise buildings. The ductility of masonry shear wall under in-plane lateral load is the ability of the panel to undergo large inelastic deformations without showing any appreciable reduction in the lateral load-carrying capacity. This fact can be established through extensive experimental investigations. This concept is equally applicable to reinforced as well as unreinforced masonry. Procedures are well established for strength design with an adequate factor of safety, but the methods to compute deflections of masonry panels, estimation of stiffness degradation and ductility under cyclic loads are still the complex parameters that restrict the acceptance by the engineering community on a unified approach for seismic-resistant design.

Masonry shear panels are normally provided with reinforced bands around the periphery and openings in the form of tie columns and bond beams. These bands are not the principle load-carrying members, but they will help to improve the integral action of the masonry wall. The improvement in ductility characteristics and shear strength helps to avoid brittle failures, particularly when the shear wall is subjected to high-intensity in-plane forces due to seismic action. Very few experimental investigations discuss the ductility concept of confined shear panels in a unified approach followed in a RC structure (Shing *et al.* 1991).

Luisa *et al.* (2004) carried out finite element analysis on shear behaviour of masonry panel under shear loading. Two different damage models were used in the analysis, namely, the isotropic model to simulate the behaviour of mortar in the micro-modelling approach and the orthotropic model to reproduce the non-linear behaviour of masonry in the macro-modelling. Barron and Hueste (2004) studied the diaphragm effect in rectangular reinforced concrete building. Under seismic loading, floor and roof systems in RC buildings act as diaphragms to transfer lateral earthquake loads to the vertical force resisting systems. The impact of in-plane diaphragm deformation on the structural response of RC building is evaluated using a performance based approach. Gabor *et al.* (2006) conducted numerical and experimental analysis of the in-plane shear behaviour of hollow brick masonry panels. The non-linear behaviour of masonry is modelled by considering perfectly elastic plastic behaviour of the mortar joint. Brasile *et al.* (2007) presented a numerical strategy based on a multilevel approach for the nonlinear analysis of brick masonry walls as in-plane prototypes of large masonry structures. Chaimoon and Attard (2007) presented a numerical formulation for the analysis of unreinforced masonry walls under shear compression fracture. The finite element formulation is based on a triangular unit constructed from constant strain triangles, with nodes along its sides but not at the vertex or at the centre of the unit. Mohamad *et al.* (2007) conducted experiments on hollow concrete block masonry prisms under compression. It was observed that mortar is responsible for the non linear behaviour of masonry. Chaimoon and Attard (2009) investigated the failure and post-peak behaviour of masonry panels with low bond strength mortar under three-point bending (TPB) both experimentally and numerically. Full-scale masonry panels with two different mortar strengths were tested under TPB. Calderini *et al.* (2010) analysed the mechanical meaning, the experimental

evaluation and the proper use of the mechanical parameters, on which the most diffused simplified models for the prediction for the diagonal cracking failure mode in masonry piers are based on. A procedure to obtain a mean evaluation of the cohesion and the friction coefficient of mortar joints of masonry through the diagonal compression test was proposed. Lipeng *et al.* (2010) proposed a constitutive law for grouted concrete block masonry in plain stress state condition.

1.1 Present investigation

Extensive investigation has been carried out on various aspects of hollow concrete block masonry panels. The investigation includes:

- (1) Unit compressive strength of hollow block, compressive strength of ungrouted and grouted hollow concrete block (HCB) prism, flexural strength of HCB prism
- (2) In-plane behaviour of HCB wall panel with and without opening under lateral load
- (3) Finite element analysis of HCB wall panel with and without opening

2. Compressive strength of hollow concrete block

The strength of masonry wall depends on many parameters, namely, the strength of individual unit, strength of mortar, joint thickness, type of construction (bonding), workmanship etc. The ultimate strength of masonry prism is always less than the individual unit strength due to composite action.

2.1 Compressive strength of unit hollow concrete block

There are many types of hollow concrete blocks varying with the grade of concrete mix used in the manufacture and in dimensions of the block. Throughout this experimental program, standard blocks from the same production plant were selected. The standard dimensions of the block are as follows:

- Size of the Full hollow concrete block : 390 mm (Length) × 190 mm (Width) × 190 mm (Height)
- Number of cores : 2
- Core size at top : 135 mm (Length) × 125 mm (Width)
- Core size at bottom : 115 mm (Length) × 100 mm (Width)
- Percentage of solids : 55
- Dimension tolerance : 3 mm
- Water absorption : 3-5%

The full size hollow concrete block was shaped at its ends to accommodate the mortar in a vertical groove and a plain surface was provided to lay the block in horizontal position over a cement mortar. In addition to the full size blocks, additional units, such as, half blocks and U-blocks of the same quality were also used in the masonry wall construction. The compressive strength of unit block and prisms were evaluated as per IS: 1905-1987. In order to obtain the modulus of elasticity of the hollow concrete blocks, 3 units, were instrumented with two sets of pellets at 100 mm gauge length on each longitudinal face of block. Using a mechanical pfender strain gauge, strains were recorded for each incremental load. The compressive strengths were calculated based on the net cross sectional area of the block. Initially, the average compressive strength of all the test samples

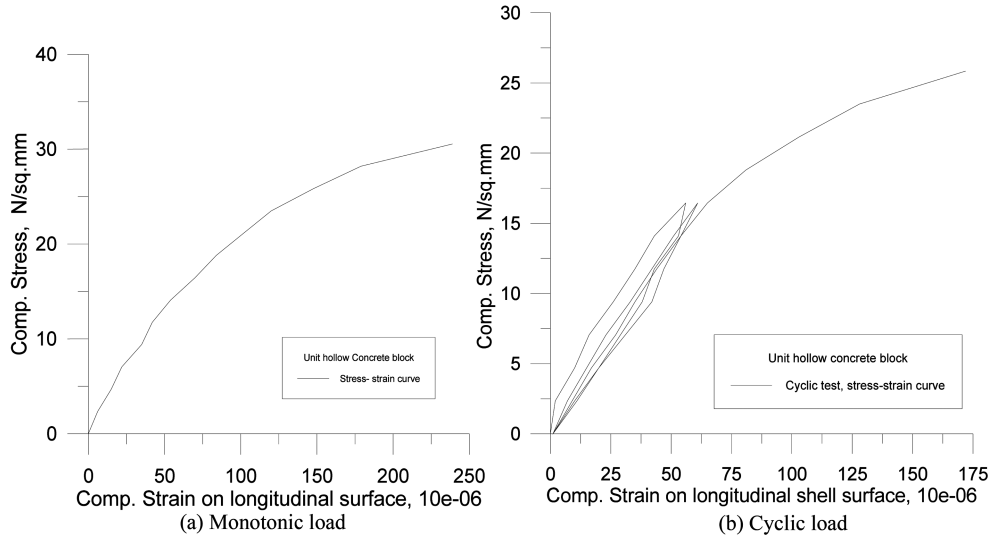


Fig. 1 Typical compressive stress-strain curve of unit hollow concrete block

was calculated. The few test samples fall beyond $\pm 15\%$ of the mean strength were not considered. Standard deviation and characteristic strength values were evaluated. Mean compressive strength, standard deviation and characteristic compressive strength of unit HCB are 33.99 Mpa, 2.27 Mpa and 30.23 Mpa respectively. The typical stress-strain curve of the unit block under direct compression is shown in Fig. 1(a). The typical cyclic stress-strain curve under loading and unloading is also shown in Fig. 1(b). At the end of two cycles of load reversals (cyclic load was limited to about 50% of the ultimate load), the specimen was tested for its ultimate compressive strength. The average modulus of elasticity of the hollow concrete block was found to be 2.497×10^4 N/mm 2 .

2.2 Compressive strength of ungrouted HCB prism

The compressive strength of the prisms was evaluated as per IS: 1905-1987. Two aspect ratios of the prism (height to thickness ratios, 2 and 3) and four mortar mixes (cement:sand - 1:3, 1:4, 1:5, 1:6) were considered. For each category (aspect ratio (h/t) and mortar mix) several numbers of ungrouted hollow concrete block prisms were fabricated. The testing and evaluation were carried out as per the procedure given in Appendix of IS: 1905-1987. The failure load for all the prisms was recorded. The compressive strengths were calculated based on net cross sectional area of the prism and the values were corrected by multiplying with the factors given in IS: 1905-1987. The statistical parameters such as mean strength, standard deviation and characteristic strength values were also evaluated as per the procedure outlined in the code. Table 1 shows the compressive strength values and statistical parameters for aspect ratio 2 and 3 and for various mortar mixes. It was observed that the mix of binding mortar and the aspect ratio have no significant variation in ultimate compression failure load of the HCB prisms. Only 1/3rd of the unit block compressive strength can be realised under prism strength value. The reduction in prism strength with height is related to shrinkage of the concrete infill and to the degree of restraint offered by the core shape, which result in plastic cracking as shrinkage proceeds. The reduction in prism strength may also be attributed to the influence of the horizontal confinement stresses exerted on the mortar joint by the

Table 1 Compressive strength results of ungrouted HCB prisms

Mortar mix	Mean comp. stress \bar{x} , standard deviation σ_{n-1} , Characteristic Comp. strength f_{ck} , and Basic Comp. stress, f_m (N/mm ²)#	\bar{x} , σ_{n-1} , f_{ck} , Basic Comp. stress, f_m (N/mm ²)@
1:3	$\bar{x} = 12.21$, $\bar{\chi}_c = k \times \bar{x} = 12.21$ $\sigma_{n-1} = 0.99$, $f_{ck} = 10.56$ $f_m = 0.25 \times f_{ck} = 2.64$	$\bar{x} = 14.30$, $\bar{\chi}_c = k \times \bar{x} = 17.16$ $\sigma_{n-1} = 1.67$, $f_{ck} = 14.40$, $f_m = 0.25 \times f_{ck} = 3.60$
1:4	$\bar{x} = 13.495$, $\bar{\chi}_c = k \times \bar{x} = 13.495$ $\sigma_{n-1} = 1.662$, $f_{ck} = 10.75$, $f_m = 0.25 \times f_{ck} = 2.688$	$\bar{x} = 13.285$, $\bar{\chi}_c = k \times \bar{x} = 15.94$ $\sigma_{n-1} = 1.336$, $f_{ck} = 13.734$, $f_m = 0.25 \times f_{ck} = 3.433$
1:5	$\bar{x} = 13.55$, $\bar{\chi}_c = k \times \bar{x} = 13.55$ $\sigma_{n-1} = 0.742$, $f_{ck} = 12.324$ $f_m = 0.25 \times f_{ck} = 3.048$	$\bar{x} = 14.54$, $\bar{\chi}_c = k \times \bar{x} = 17.44$ $\sigma_{n-1} = 1.25$, $f_{ck} = 15.38$, $f_m = 0.25 \times f_{ck} = 3.845$
1:6	$\bar{x} = 13.42$, $\bar{\chi}_c = k \times \bar{x} = 13.42$ $\sigma_{n-1} = 0.271$, $f_{ck} = 12.92$ $f_m = 0.25 \times f_{ck} = 3.24$	$\bar{x} = 12.85$, $\bar{\chi}_c = k \times \bar{x} = 15.42$ $\sigma_{n-1} = 0.756$, $f_{ck} = 14.17$, $f_m = 0.25 \times f_{ck} = 3.549$

values corresponding to aspect ratio = 2 and

@ is for aspect ratio = 3

stiff concrete blocks and the small thickness of the mortar joint relative to the height of the block.

2.3 Compressive strength of grouted HCB prisms

In order to increase the load carrying capacity of hollow block masonry, the cores were grouted i.e., filled with concrete. If the masonry is to resist moments due to lateral loads or seismic forces in addition to axial loads, suitable reinforcements are to be embedded in the concrete grout. Grouting is also resorted to, for local strengthening under concentrated loads or around openings. For grout specification and testing, ASTM C 476 and UBC Standard No. 21-19 are usually referred (UBC 1994). Several numbers of HCB prisms were cast for each aspect ratio (h/t) of 2 and 3. The grout mix and mortar mix were 1:2:3 (by weight) and 1:5 respectively, with water-cement ratio of 0.6 and super plasticizer of 0.5 litre/100 kg of cement. The compressive strengths were calculated based on gross cross sectional area of the prism. The compressive strengths were corrected by multiplying

Table 2 Compressive strength results of grouted HCB prisms

Mean comp. stress \bar{x} , standard deviation σ_{n-1} , Characteristic Comp. strength f_{ck} , and Basic Comp. stress, f_m (N/mm ²)#	\bar{x} , σ_{n-1} , f_{ck} and Basic Comp. stress, f_m (N/mm ²)@
$\bar{x} = 15.33$, $\bar{\chi}_c = k \times \bar{x} = 15.33$ $\sigma_{n-1} = 0.75$, $f_{ck} = 14.09$ $f_m = 0.25 \times f_{ck} = 3.523$	$\bar{x} = 13.12$, $\bar{\chi}_c = k \times \bar{x} = 15.74$ $\sigma_{n-1} = 1.138$, $f_{ck} = 13.86$ $f_m = 0.25 \times f_{ck} = 3.465$

values corresponding to aspect ratio = 2 and

@ is for aspect ratio = 3



Fig. 2 Failure pattern of grouted HCB prism

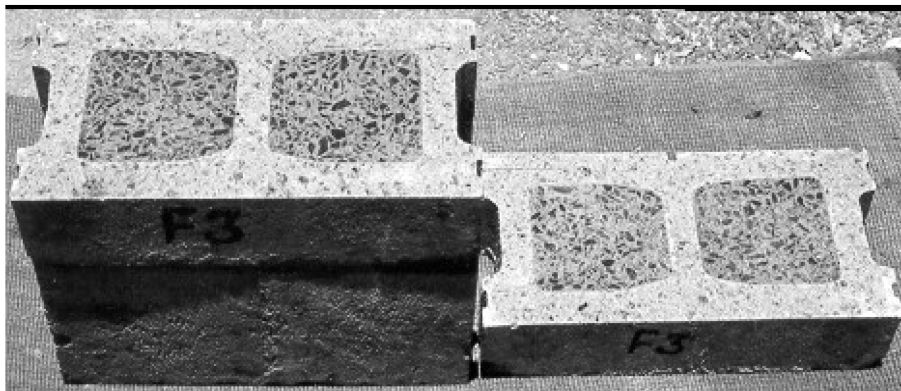


Fig. 3 Cut view of HCB grouted prism for aspect ratio = 3.0

with the factors given in IS: 1905-1987. Mean strength, standard deviation and characteristic strength values were evaluated. Table 2 shows the results of compressive strength for grouted hollow concrete block prisms for aspect ratio 2 and 3.

From Tables 1 and 2, it can be observed that the compressive strength of HCB prisms having aspect ratio 2 is about 10% higher compared to ungrouted HCB prism. Typical failure pattern of the grouted hollow concrete block prism is shown in Fig. 2. In all the grouted prisms, the bond between the grout and hollow concrete block core was found to be good. The cross section view of the cut grouted prism (Fig. 3) shows the developed grout mix provides better bond characteristics, which improves the performance of masonry panel under lateral and vertical loads. By comparing the ungrouted and grouted compressive strength results (refer Tables 1 and 2), it can be inferred that the grout is optimally designed for the corresponding strength of HCB unit block. It can be observed from Table 2 that there is no significant variation in compressive strength for aspect ratio 2 and 3.

Table 3 Flexural tensile strength of grouted hollow concrete block prisms

Loading	Avg. flexural tensile stress and standard deviation
Two point	$\bar{x} = 3.08 \text{ N/mm}^2$ $\sigma_{n-1} = 0.502 \text{ N/mm}^2$
Central	$\bar{x} = 4.30 \text{ N/mm}^2$ $\sigma_{n-1} = 0.0 \text{ N/mm}^2$

3. Flexural strength of hollow concrete block prisms

Walls are frequently subjected to lateral loads as well as moments due to eccentric gravity loads. Hence, there is a need to consider the strength of masonry under flexure. Flexural bond strength may be used as a measure of the bonding between two masonry materials (block/brick and mortar). Masonry flexural strength is tested by using small prisms under four point or three point bending.

The strength of conventional masonry in flexure with stress perpendicular to bed joints is determined by the bond between masonry units and mortar, because bond strength is almost invariably lower than the tensile strength of the masonry units or of the mortar. The mortar mix used was 1:5, the concrete mix and water cement ratio were 1:2:3 and 0.6. Super plasticizer added to the mix was 0.5 lit/100 kg of cement. Several prisms were tested under equal concentrated loads at the span third points and were under central point. Table 3 shows the result of flexural strength of hollow concrete block prisms. The mean flexural strength and standard deviation were evaluated for the two types of loading conditions. It can be observed that (refer Tables 1 and 2) flexural strength of the HCB prisms is about 25% of the compressive strength of prism.

4. Studies on shear walls

4.1 Test 1

In seismic resistant design of shear walls, both the strength and ductility are the important factors to be evaluated. Many experimental investigations in the past were carried out to understand the behaviour of masonry panels under compressive loads. The compressive strength of the wall panel depends on the strength of the unit, strength of mortar, slenderness ratio and eccentricity of axial

Table 4 Details of HCB wall panel with and without opening

Type of confined panel/code with reinforcement and grout	Size of panel $1 \times t \times h, m$	No. of tie columns	Vertical steel area, mm^2	% of shear area	h/l	
Fully reinforced and grouted	FR-HCB	$1.6 \times 0.19 \times 1.2$	8-1-12#	904.8	0.30	0.75
Partially grouted	PR1-HCB	$1.6 \times 0.19 \times 1.2$	4-1-12#	452.4	0.15	0.75
Partially reinforced fully grouted	PR2-HCB	$1.6 \times 0.19 \times 1.2$	4-1-12#	452.4	0.15	0.75
Ungrouted	UR-HCB	$1.6 \times 0.19 \times 1.2$	-	-	-	0.75
HCB panel with opening 1.8×1.0	OP-HCB	$2.2 \times 0.2 \times 2.5$	4-1-12# 1-1-12#	452.4	0.10	1.14

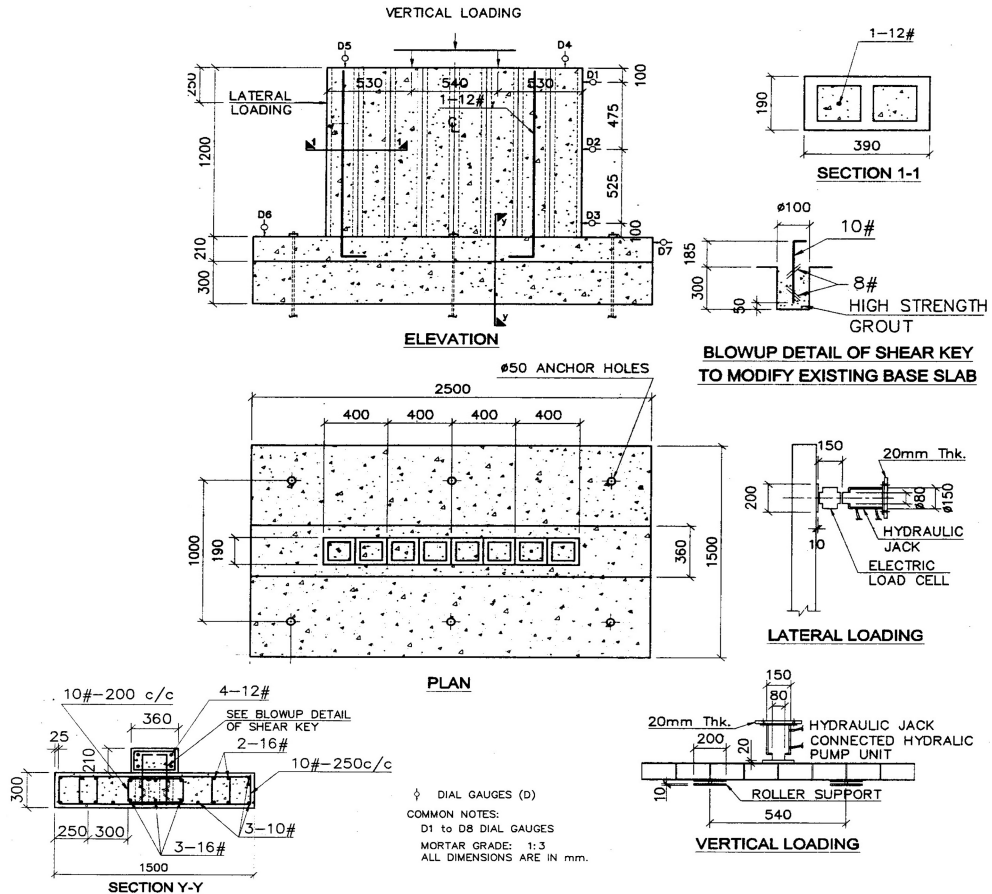


Fig. 4 Details of partially reinforced and fully grouted HCB wall panel-without opening

load. Very limited experimental work has been carried out on the behaviour of panel under lateral load. The ductility behaviour of shear wall is the primary factor, considered in aseismic strength design. In this experimental programme, displacement ductility indices were derived for the following three types of construction schemes, namely, unreinforced masonry panel, partially reinforced panel and fully reinforced panel. Table 4 shows the details of tested HCB wall panels with and without opening. Fig. 4 shows the typical plan, elevation and instrumentation details of HCB wall panel without opening.

4.2 Testing of HCB wall panels

Vertical load was applied through hydraulic jack of capacity 20 t. In this, hydraulic pressure could be maintained at the discrete load intervals through a hydraulic plant. Lateral load was applied through a manually operated hydraulic jack. The lateral load was recorded by a proving ring, which has the least count of 135 kg/division. For some wall panels, lateral load was applied through an electric load cell. Initially, the vertical load was increased in the steps of 1.0 t upto the maximum load of 10 t. This load of 10 t is the maximum estimated vertical load, considering the dead load of

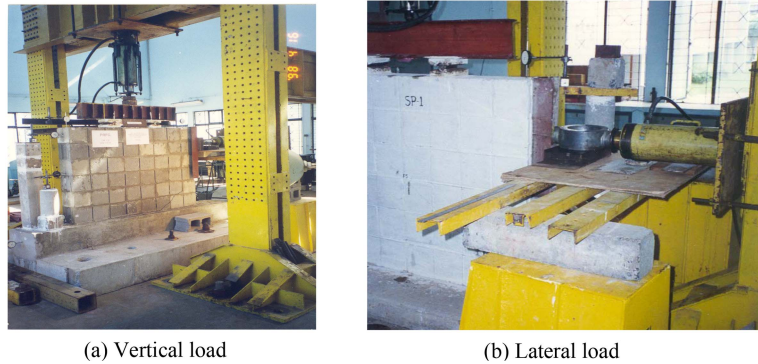


Fig. 5 Typical test set up of HCB – without opening

panels and a part of live load in a low rise building, was kept constant for all the specimens. Higher axial load on the wall tends to improve the sliding friction and hence beneficial from stability aspect under lateral load. The lateral load was increased in the incremental manner upto the failure of the specimen. The typical test set up including dial gauge positions is shown in Fig. 5. Axial strains and shear strains were measured by means of a mechanical pfender gauge. Dial gauges were placed at selected locations to measure the vertical as well as lateral deformations. The least count of the dial gauge is 0.01 mm. Along with the displacement measurements, the crack pattern was also recorded. Fig. 6 shows the typical failure details of fully grouted and partially reinforced wall panel (PR2-HCB). Fig. 7 shows the failure pattern details of HCB wall panel with opening (OP-HCB). The



Table 5 Displacement ductility factors of masonry panels obtained from monotonic tests

No.	Construction scheme	Displacement ductility ratio	Load at yield deformation, P_y	Load at ultimate deformation, P_u	Load ratio, P_u/P_y	R_{st}	R_{cy}
1	UR-HCB	1.94	7.10	9.37	1.32	2.56	1.02
2	PR1-HCB	2.57	9.37	15.41	1.64	4.21	1.68
3	PR2-HCB	4.50	9.37	19.0	2.03	9.13	3.65
4	FR-HCB	5.98	15.50	17.20	1.11	6.64	2.66
5	OP-HCB	3.14	6.19	6.35	1.03	3.23	1.29

failure pattern at the ultimate load stage of HCB panels showed a dominant strut action. The crack widths were limited and a dominant diagonal crack is noticed along the joints towards compression toe. Larger deformation may be obtained by improving the tension resisting capacity. The ductility behaviour under lateral loads of unreinforced panels can be substantially improved by providing vertical reinforcement. The fully reinforced panels yield 100% higher ultimate deformations as compared to unreinforced panels.

Designing the structural element to remain within the elastic state is not economically feasible under seismic loading. Hence, by considering the equivalent energy approach, the displacement ductility ratio derived from elasto-plastic mechanism can be advantageously used for economical design. The resistance required for the element is inversely proportional to the ductility derived. Hence, the ductility indices and the overstrength factors are the two primary factors that need consideration in capacity design approach of seismic resistant design. The two factors namely, strength factor (P_u/p_y), and displacement ductility factors (Δ_U), are to be realistically assessed through an experimental work, since they depend upon material characteristics and detailing. In this experimental programme, by idealising the load and deformation plot as an elasto-plastic curve, and considering the secant stiffness approach, the displacement ductility indices and over strength factors were determined. For all the panels, the ultimate deformation was considered at a displacement value corresponding to the significant load drop beyond 20%. In few cases, the abrupt failure of the panel was noticed and the ultimate deformation was considered corresponding to the peak load. The yield deformation for all panels of the same type was derived by secant stiffness approach. Table 5 shows the derived displacement ductility indices for various panels under monotonic lateral load. The performance of reinforced HCB panels is much superior at the ultimate stage, as its performance is similar to that of RC wall. The influence of vertical reinforcement is significant in improving the ductility behaviour. The response reduction factors (derived from static tests – R_{st}) increases with the amount of vertical reinforcement and grout volume. The ductility indices for reinforced concrete members with short span shear ratio (predominant shear and flexure influence), derived under cyclic load tests may decrease the indices to 40% as that of the indices obtained from static tests (Srinivasa Rao *et al.* 1998). Extending this concept to take into account the cyclic load effect, the response reduction factors (R_{cy}) can be worked out and are given in Table 5.

5. Finite element analysis

Masonry structural components require understanding into the responses of those components to a variety of loadings. There are number of methods for modelling the structures/components through

numerical approaches such as analytical and finite element method. Finite element analysis (FEA) is one of the numerical techniques widely employed to engineering design applications.

5.1 Finite element modelling issues

A large number of different FE formulations have been used for the analysis of concrete structural components. These may be categorized into facet plate/shell elements, thin-shell elements (Kirchoff assumptions), thin/thick shell elements (Reissner-Mindlin theory) and three dimensional elements. The choice of an element for analysis of a structure/component depends on the geometry and the purpose for which the results of the analysis are to be used. Accurate numerical analysis of masonry panels including lateral loadings has to be based on a three dimensional model. This requires considerable computational effort in terms of simulating test conditions as close as possible. The following are some of the key aspects w.r.t modelling of reinforced hollow concrete block:

- FE modelling of HCB wall panel including reinforcement
- Material modelling of concrete and steel
- Various loads for modelling such as compression load and lateral load
- Employing appropriate elements such as link and solid for effective load transfer and to simulate the realistic behaviour
- Simulation of material nonlinearity for larger load steps and post yield/crack regime.

5.2 Material nonlinearity

When a large force is applied on the structure/component, the resulting stresses may be greater than the yield strength of the material. In such a case, multilinear stress-strain relationship of the material can be used to consider the plastic deformation of the material. Key concepts in modelling inelastic behavior in general may include:

- The decomposition of strain into elastic and plastic parts
- Yield criterion to predict whether the solid responds elastically or plastically
- Strain hardening rules, which control the shape of the stress-strain curve in the plastic regime
- The plastic flow rule, which determines the relationship between stress and plastic strain

However, considering the inherent uncertainties involved in determining some of the key parameters stated above, use of multi linear stress strain behaviour for grouted masonry and steel obtained in test programme have been used for the analysis.

The elastic unloading criterion, which models the irreversible behaviour

5.3 FE Modelling and analysis of HCB wall panel with and without opening

Creation of geometry and finite element mesh, modelling of all loads, defining material properties, simulation of material nonlinearity and application of boundary conditions were carried out by using a general purpose finite element software, ANSYS 6.0 (2002). The details of modelling are furnished below. Volume was created as per the geometry shown in Fig. 4. FE mesh along with model characteristics is shown in Fig. 8. A eight-noded solid element (Solid 65) is used to model the concrete with or without reinforcing bars. The solid element has eight nodes with three degrees of freedom at each node translations in the nodal x, y and z directions. The element is capable of plastic deformation cracking in three orthogonal directions and crushing (refer Fig. 9).

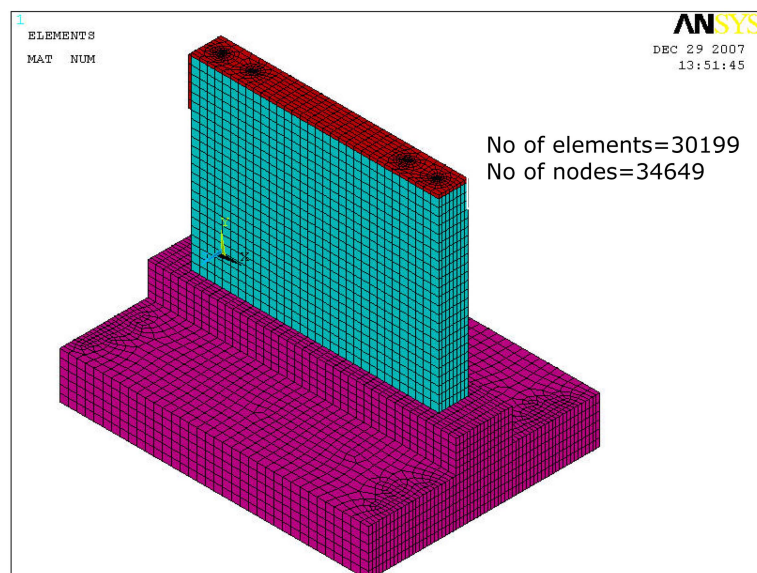


Fig. 8 FE model and characteristics

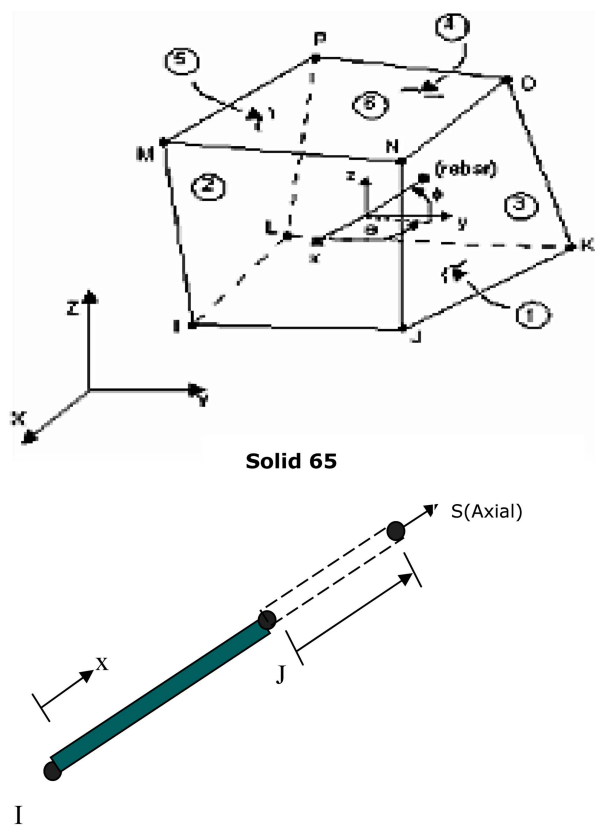


Fig. 9 FE elements used for modelling

Link element is used to model the reinforcement. The 3-D spar element (link element) is a uniaxial tension-compression element with three degrees of freedom at each node: translations in the nodal x , y and z directions (refer Fig. 9). This element has plasticity, creep, swelling, stress stiffening and large deflection capabilities. Further, the stiffening and large deformation capability are of interest in modelling steel reinforcement.

5.3.1 Material properties

Material properties for the concrete and steel are given in Table 6. For linear static analysis, modulus of elasticity and poisson's ratio are the input values whereas for nonlinear static analysis, multilinear elastic model available in ANSYS have been used. The material behavior is described by a piece-wise linear stress-strain curve, starting at the origin, with positive stress and strain values. Successive slopes can be greater on lower than the preceding slope; however, no slope can be greater than the elastic modulus of the material. In the present case, successive slopes are lower than the proceeding slope. The slope of the first curve segment usually corresponds to the elastic modulus of the material, although the elastic modulus can be input as greater than the first slope to

Table 6 Material properties

	<ul style="list-style-type: none"> • Modulus of elasticity = 24970 MPa Poisson's ratio, $\nu = 0.12$ Shear transfer coefficients for an open crack = 0.2 Shear transfer coefficients for a closed crack = 0.9 Uniaxial tensile cracking stress = 2.5 MPa • Uniaxial crushing stress = 25 MPa Biaxial crushing stress = 0.0 Ambient Hydrostatic stress state = 0.0 Biaxial crushing stress under ambient hydrostatic stress state = 0.0 Uniaxial crusing stress under ambient hydrostatic stress state = 0.0 Stiffness multiplier for cracked tensile condition = 0.0 • Some of the parameters given above are default values, which will be modified by input stress-strain curves.
Masonry	Modulus of elasticity = 20000 MPa, Poisson's ratio = 0.3
Steel	

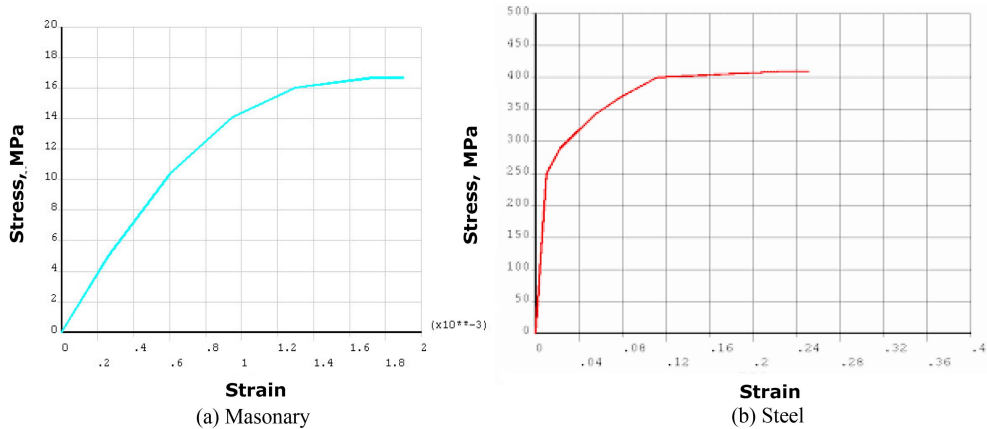


Fig. 10 Multi-linear stress strain plots

ensure that all slopes are less than or equal to the elastic modulus. Fig. 10 shows multilinear stress strain plot adopted for steel and concrete material. Stress strain plot adopted for masonry is the same as that obtained from experiments on grouted prisms (refer Fig. 1).

5.3.2 Loading and boundary conditions

Constant vertical load of 10 t is applied on the top of wall panel and incremental lateral load is applied horizontally. All the degree of freedom at the bottom of the wall panel were constrained.

Newton-Raphson procedure was employed for nonlinear static analysis where the load is divided into series of load increments applied in several load steps. Before each solution step, out-of-balance load vector which is the difference between the restoring forces corresponding to element stresses and the applied load is evaluated. Then a linear solution is carried out using out-of-balance loads and convergence is checked. When the convergence criterion is not satisfied, out-of-balance load is reevaluated, the stiffness matrix is updated and a new solution is obtained. This iterative procedure is

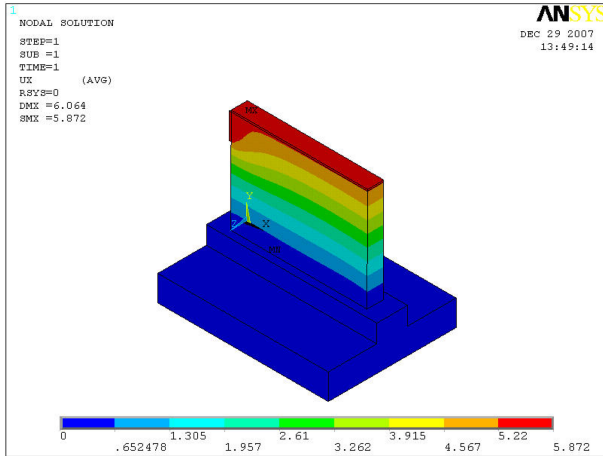


Fig. 11 In-plane (U_x) displacement contour

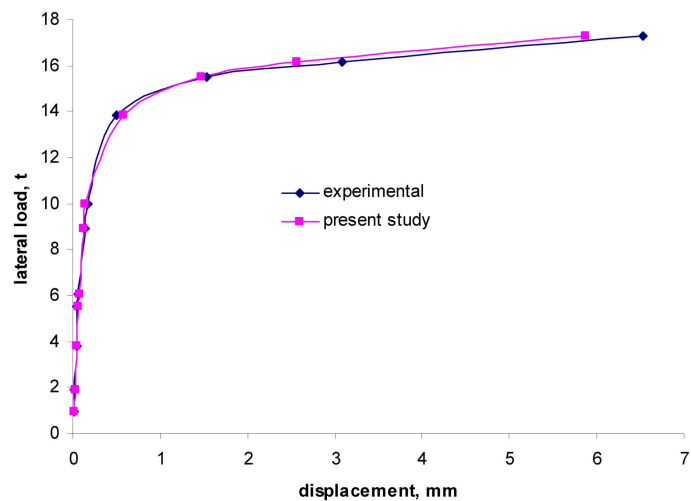


Fig. 12 Lateral load vs displacement

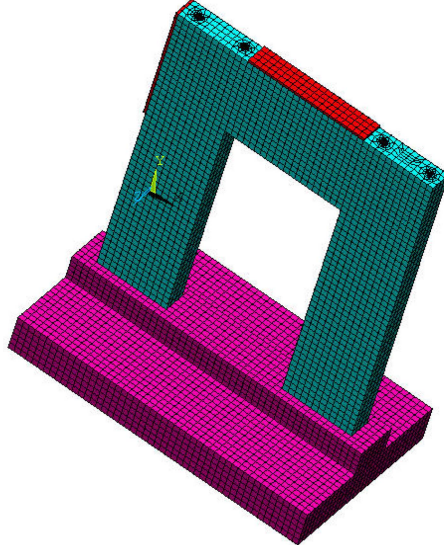


Fig. 13 FE mesh of wall panel with opening

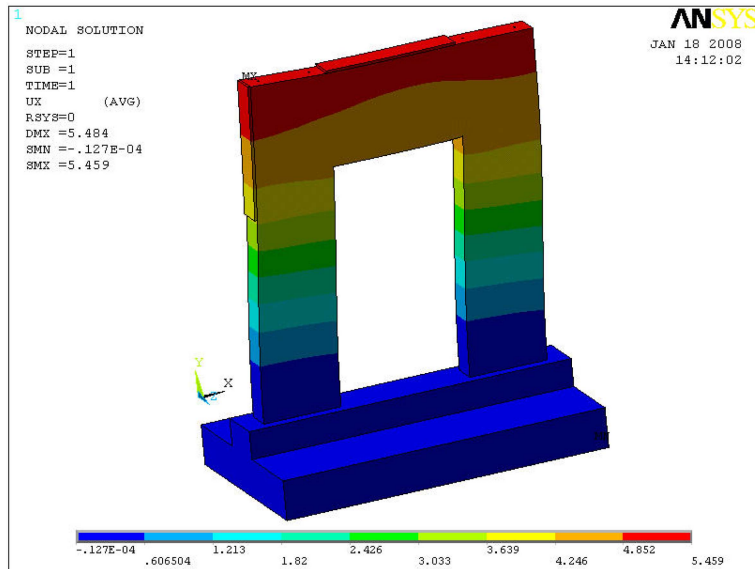


Fig. 14 In-plane displacement contour (OP-HCB)

continued until the solution converges.

5.3.3 Analysis

Linear static and nonlinear static analysis was carried out depending on the magnitude of lateral load for FR-HCB specimen.

Fig. 11 shows the in-plane displacement contour corresponding to the ultimate lateral load of $17.26 t$.

Fig. 12 shows the plot of computed in-plane displacement values and the corresponding experimental observations. From Fig. 12, it can be observed that the computed values are in very good agreement

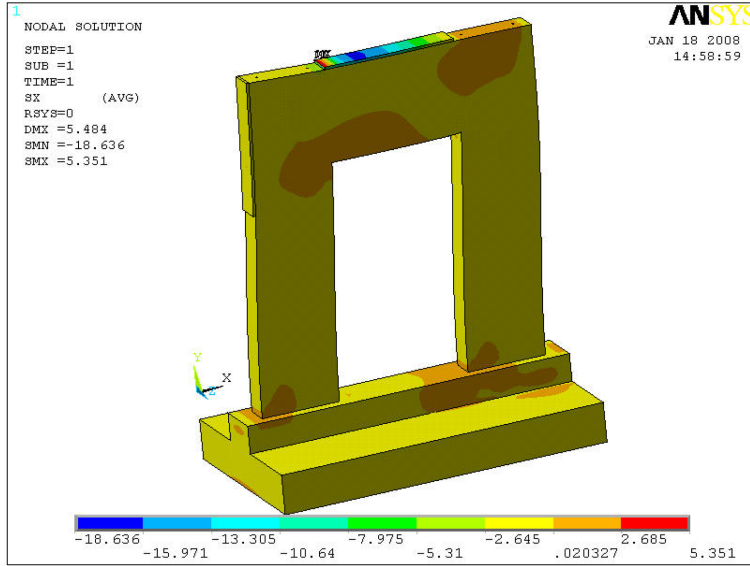


Fig. 15 σ_x Stress contour (OP-HCB)

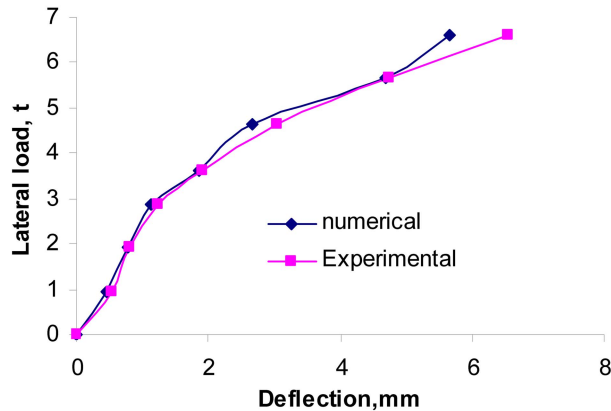


Fig. 16 Lateral load vs displacement (OP-HCB)

with the corresponding experimental observations.

Fig. 13 shows the finite element modelling of reinforced hollow concrete block masonry wall panel with opening. Fig. 14 shows the in-plane deformation contour for the ultimate lateral load of 6.62 t. Stress contour (σ_x) is shown Fig. 15. From Fig. 15, it can be observed that one of the corners of the opening experiencing maximum stress. Fig. 16 shows the plot of computed in-plane deformation and the corresponding experimental observation for different magnitudes of lateral load. From Fig. 16, it can be observed that there is very good agreement between them.

6. Conclusions

It is known that seismic resistance design of masonry buildings requires reinforced masonry

construction to prevent sudden collapse and minimize damage. From the wide literature review, it was observed that the research carried out on the shear walls made up of hollow concrete masonry blocks is limited.

Extensive research study was carried out on hollow concrete block masonry units and wall panels. The study includes, compressive strength of unit block, ungrouted and grouted HCB prisms, flexural strength evaluation and testing of HCBM panels with and without opening. Non-linear finite element analysis was also carried out to compare the deformations under each incremental lateral load. The mortar joint was not modelled separately. Equivalent multilinear stress strain variation was considered for the grouted HCBM and steel.

Displacement ductility factors and response reduction factors were evaluated based on experimental results. From the study, it is observed that fully grouted and partially reinforced HCBM panel without opening performed well compared to other types of wall panels in lateral load resistance and displacement ductility. In all the wall panels, shear cracks originated at loading point and moved towards the compression toe of the wall. The force reduction factor of a wall panel with opening is much less when compared with fully reinforced wall panel with no opening. The in-plane displacement values obtained by non-linear FE analysis are found to be in good agreement with the corresponding experimental values for reinforced HCBM. The derived response reduction factors will be useful for adopting elasto-plastic design procedures for the lateral forces generated due to earthquakes

Acknowledgments

Authors would like to thank Mr. HG Sreenath, Former Deputy Director, SERC, Dr. B. Sivarama Sarma, Head R&D, L&T, Chennai and V. Vimalanandam, Former Assistant Director, SERC for their valuable suggestions. Authors would also like to thank Building Materials & Technology Promotion Technology Council, New Delhi for sponsoring the project to carry out experimental investigation. The study is being published with the approval of the Director, Structural Engineering Research Centre, Chennai, India.

References

- ANSYS 6.0 (2002), Theory and Reference Manual.
- Calderini, C., Cattari, S. and Lagomarsino, S. (2010), "The use of the diagonal compression test to identify the shear mechanical parameters of masonry", *Constr. Build. Mater.*, **24**(5), 677-685.
- Chaimoon, K. and Mario, M. Attard (2009), "Experimental and numerical investigation of masonry under three-point bending (in-plane)", *Eng. Struct.*, **31**(1), 103-112.
- Gabor, E., Ferrier, E., Jacquelain and Hamelin, P. (2006), "Analysis and modelling of the in-plane shear behavior of hollow brick masonry panels", *Constr. Buil. Mater.*, **20**(5), 308-321.
- Gihad Mohamad, Paulo B. Lourenco and Humberto R. Roman. (2007), "Mechanics of hollow concrete block masonry prisms under compression: Review and prospects", *Cement Concrete Comp.*, **29**(3), 181-192.
- IS: 1905-1987, *Code of Practice for Structural Use of Unreinforced Masonry*, 3rd Edition, Bureau of Indian Standards, New Delhi, India.
- Joel, M. Barron. and Mary Beth D. Huste. (2004), "Diaphragm effects in rectangular reinforced concrete buildings", *ACI Struct. J.*, **101**(5), 615-624.
- Krit, Chaimoon and Mario, M. Attard. (2007), "Modeling of unreinforced masonry walls under shear and

- compression”, *Eng. Struct.*, **29**(9), 2056-2068.
- Liu, Lipeng, Wang, Zonglin, Zhai, Changhai and Zhai, Ximei (2010), “Constitutive law of grouted concrete block masonry in plain stress state”, *Struct. Eng. Mech.*, **34**(3), 391-394.
- Luisa Berto, Anna Saetta, Roberto Scotta and Renato Vitaliani. (2004), “Shear behaviour of masonry panel: parametric FE analyses”, *Int. J. Solids Struct.*, **41**(16-17), 4383-4405.
- Sandro Brasile, Raffaele Casciaro and Giovanni Formica. (2007), “Multilevel approach for brick masonry walls- Part I: A numerical strategy for the nonlinear analysis”, *Comput. Method. Appl. M.*, **196**(49-52), 4934-4951.
- Shing, P.B., Noland, J.L., Spaeh, H.P., Klammerus, E.W. and Schuller, M.P. (1991), “Response of single-story reinforced masonry shear walls to in-plane lateral loads”, *Report No 3.1 (a)-2, U.S. Japan Coordinated Program for Masonry Building Research*.
- Srinivasa Rao, P., Sivarama Sarma, B., Lakshmanan, N. and Stangenberg, E. (1998), “Damage model for reinforced concrete elements under cyclic loading”, *ACI Mater. J.*, **95**(6), 682-690.
- UBC (1994), *Uniform Building Code*, International Conference of Building Officials, Whittier, California.

CC